LONDON, METEOROLOGICAL OFFICE.

Met.O.19 Branch Memorandum No. 30.

The determination of stratospheric aerosol number densities from a laser inelastic scattering experiment. By SLINGO, A.

London, Met.Off., Met.O.19 Br.Memo.No.30, 1976, 30cm.Pp.[14].5 Refs.

An unofficial document - restriction on first page to be observed.

THE DETERMINATION OF STRATOSPHERIC AEROSOL NUMBER DENSITIES FROM A LASER INELASTIC SCATTERING EXPERIMENT

A. SLINGO

March 1976

1. INTRODUCTION

The laser inelastic scattering experiment at Beaufort Park operates at two wavelengths - 465 nm and 605 nm (Pettifer 1975). In principle it is possible to recover information on aerosols at a given height in the stratosphere from the ratio of the number of photons back-scattered at each frequency (Pettifer, equation 2-24);

$$\frac{P(\lambda_1, Z)}{P(\lambda_2, Z)} = \frac{P_o(\lambda_1)\,T^2(\lambda_1)\;Q(\lambda_1)}{P_o(\lambda_2)\,T^2(\lambda_2)\;Q(\lambda_2)}\left\{\frac{\rho(Z)\,B(\lambda_1) + A(\lambda_1)}{\rho(Z)\,B(\lambda_2) + A(\lambda_2)}\right\} \quad (1)$$

Where $P(\lambda, Z)$ is the number of back-scattered photons at wavelength λ from the height Z.

$P_o(\lambda)$ is the number of transmitted photons.

$T(\lambda)$	transmission of the atmosphere up to height Z.
$Q(\lambda)$	efficiency of the receiver.
$\rho(Z)$	molecular (i.e. air) number density at Z.
$B(\lambda)$	molecular back-scatter cross-section per steradian
$A(\lambda)$	contribution from the aerosols at Z.

The contribution to $T(\lambda)$ from the aerosols between the ground and the level of interest is ignored as most of the scattering takes place in the lowest atmospheric layers.

The scattering from air molecules, as described by the terms $\rho(Z)B(\lambda_1)$ and $\rho(Z)B(\lambda_2)$, takes place in the Rayleigh regime ($\frac{2\pi m r}{\lambda} \ll 1$, where m is the refractive index, r the particle radius and λ the incident photon wavelength) so that $B(\lambda)$ is easily calculated. The physical parameters of stratospheric aerosols are such that Rayleigh theory does not describe the scattering adequately, which is why we can separate the terms $\rho(Z)B(\lambda)$ and $A(\lambda)$ and gain information on the aerosols. Previous attempts to calculate $A(\lambda)$ used the Rayleigh-Gans approximation, for which we require;

$$|m-1| \ll 1 \quad \text{and} \quad \frac{4\pi r}{\lambda}|m-1| \ll 1 \qquad (2)$$

Since λ is fixed and m could easily be as high as 1.5, this places an upper limit to the size of the particle whose scattering is described adequately;

$$\text{At } 605 \text{ nm} \qquad r \ll 0.1\ \mu\text{m} \tag{3}$$

This is far too low when compared to measured size distributions (see section 2) so that $A(\lambda)$ must be found using the more general Mie theory. Because of the complexity of the calculations required to determine the Mie functions it was decided to use published tabulations, most of which are of the "Backscatter Gain", G, for which it can easily be shown that:

$$A(\lambda) = \frac{1}{4} \int_0^\infty G\left(m, \frac{2\pi r}{\lambda}\right) N(r)\, r^2\, dr \tag{4}$$

where for simplicity a single species of aerosol, with real refractive index m and size distribution $N(r)$, has been assumed to be present. Figure 1 shows the form of the backscatter gain as a function of refractive index and of the Mie size parameter $\alpha = \frac{2\pi r}{\lambda}$. The backscatter gain predicted by the Rayleigh-Gans approximation is also illustrated. Note that the two diverge for $\alpha \gtrsim 1$, i.e. for $r \gtrsim 0.1\ \mu$m.

2. THE "BEST FIT" SIZE DISTRIBUTION FUNCTIONS

In order to calculate $A(\lambda)$ we need to specify the size distribution function, $N(r)$. The size distributions deduced from various sampling experiments are illustrated in Figure 2, from which it will be seen that a wide range of distributions have been observed, although the general trend is for a decrease in the concentration with increasing particle size. The model distributions chosen to calculate $A(\lambda)$ are shown in Figure 3. All have the property that the total number of particles larger than 0.01 μm is 100 cm^{-3}.

Equation 4 was integrated numerically over each of the model distributions, for the two operating wavelengths, using the values of backscatter gain at $m = 1.4821$ and 1.60 given by Kerker (1969) and by Atlas et.al.(1963). In Figure 4 the results of the calculations for the Haze H function are compared with some values interpolated from the tabulations of Deirmendjian (1969), who calculated $A(\lambda)$ at 450 and 700 nm for water vapour ($m = 1.33-1.34$) and silicate ($m = 1.54 - 1.56$). The smooth variation of $A(\lambda)$ with refractive index is caused by the exponential cut-off to the haze H function, which ensures that the integral in equation 4 converges before the oscillations in G are encountered.

We now assume that the real aerosol size distribution function may, in the size range of interest, be approximated to by multiplying a given model distribution, $N(r)$, by some factor q.

The number density of particles in this new "best fit" distribution is therefore;

$$N'(r) = q\, N(r) \tag{5}$$

and because we have independent scattering this means that;

$$A'(\lambda) = q\, A(\lambda) \tag{6}$$

Then if we let $\dfrac{P(\lambda_1, Z)}{P(\lambda_2, Z)} = R(Z)$ and $\dfrac{P_o(\lambda_1)T^2(\lambda_1)Q(\lambda_1)}{P_o(\lambda_2)T^2(\lambda_2)Q(\lambda_2)} = F$ (7)

We can re-write equation (1);

$$R(Z) = F\left\{\frac{\rho(Z)\,B(\lambda_1) + q\,A(\lambda_1)}{\rho(Z)\,B(\lambda_2) + q\,A(\lambda_2)}\right\} \tag{8}$$

Whence ;

$$q = \rho(Z)\left\{\frac{\dfrac{F.\,B(\lambda_1)}{R(Z)} - B(\lambda_2)}{A(\lambda_2) - \dfrac{F.\,A(\lambda_1)}{R(Z)}}\right\} \tag{9}$$

3. APPLICATION TO REAL DATA

Equation 9 may now be used to estimate the aerosol concentration profile from real data. In table I the laser data recorded on the night of 12-13 January 1975 are listed, together with other necessary data.

The calculated values of $A(\lambda)$ have been extrapolated to a refractive index of $m = 1.4$, which lies in the range expected for aerosols in the lower stratosphere. Equation 9 was solved for each model distribution. The results for the 21 km level are presented in Figure 5. The curves give very similar results for the total number of particles with sizes between 0.1 and 1 μm because this is the range where the integrand in equation 4 is largest. For any reasonable aerosol size distribution the laser experiment is therefore most sensitive to aerosols of about this size and by the same token it cannot be used to infer the number densities well outside this range, so that the divergence of the models for $r \ll 0.1$ μm is irrelevant.

In Figure 6 the results are presented as a number density profile of aerosols with sizes between 0.1 and 1 μm. These have been derived using the Haze H function, though the profiles calculated for the other distributions are very similar in shape. The profile shows a well defined aerosol layer between 21 and 31 km, with some evidence for two more layers at around 37 km and above 43 km. Note that the simple theory breaks down if $R(Z) < F \frac{B(\lambda_1)}{B(\lambda_2)}$ or $R(Z) > F \frac{A(\lambda_1)}{A(\lambda_2)}$ when it predicts negative number densities.

Because of the expected increase with height of the extra-terrestrial content of the aerosol population, it is possible that the assumed refractive index of 1.4 is too low in the upper stratosphere. The number densities were therefore calculated again assuming $m = 1.6$. A comparison of the two sets of data at a height of 49 km is presented in Table 2.

It will be noticed that fewer particles are required to account for the data as the assumed refractive index is increased and that the dependence of the derived number densities on the refractive index increases as the relative number of large particles increases. This is due to the increasing dependence of the backscatter gain on refractive index as the region of the large oscillations in G is entered (see Figure 1).

REFERENCES

Atlas D., Battan L.J., Harper W.G., Herman B.M., Kerker M. & Matijević E. (1963). IEEE Trans.Antennas.Propagation AP-11, 68.

Cadle R.D. & Grams G.W. (1975). Reviews of Geophysics & Space Physics 13, 475.

Deirmendjian D. (1969). Electromagnetic scattering on Spherical Polydispersions, American Elsevier Publishing Co. Inc., New York.

Kerker M. (1969). The Scattering of light and other Electromagnetic Radiation, Academic Press, New York and London.

Pettifer R. (1975). Ph.D. Thesis, Queen's University of Belfast.

TABLE I

GENERAL AND LASER DATA USED TO RETRIEVE THE PROFILE OF 12/13.1.75

λ_1 = 605 nm

λ_2 = 465 nm

$B(\lambda_1)$ = $3.48 \cdot 10^{-32}$ $m^2\ sr^{-1}$

$B(\lambda_2)$ = $9.98 \cdot 10^{-32}$ $m^2\ sr^{-1}$

F = 4.30

Model distribution	$A(\lambda_2)\ m^{-1}sr^{-1}$	$A(\lambda_1)\ m^{-1}sr^{-1}$
Haze H	$3.220 \cdot 10^{-7}$	$2.344 \cdot 10^{-7}$
Power Law, ν=3	$1.033 \cdot 10^{-8}$	$1.033 \cdot 10^{-8}$
4	$4.393 \cdot 10^{-10}$	$3.377 \cdot 10^{-10}$
5	$4.175 \cdot 10^{-11}$	$2.466 \cdot 10^{-11}$
6	$6.274 \cdot 10^{-12}$	$2.849 \cdot 10^{-12}$

Height (km)	R(Z)	Molecular Number Density (cm^{-3})*
21	1.708 ± 0.02	$1.51 \cdot 10^{24}$
23	1.777 ± 0.03	$1.10 \cdot 10^{24}$
25	1.734 ± 0.04	$7.92 \cdot 10^{23}$
27	1.734 ± 0.05	$5.70 \cdot 10^{23}$
29	1.667 ± 0.06	$4.15 \cdot 10^{23}$
31	1.930 ± 0.07	$2.96 \cdot 10^{23}$
33	1.511 ± 0.09	$2.28 \cdot 10^{23}$
35	1.616 ± 0.11	$1.66 \cdot 10^{23}$
37	1.658 ± 0.13	$1.23 \cdot 10^{23}$
39	1.829 ± 0.18	$9.20 \cdot 10^{22}$
41	1.387 ± 0.15	$6.88 \cdot 10^{22}$
43	1.608 ± 0.23	$5.10 \cdot 10^{22}$
45	1.544 ± 0.23	$4.10 \cdot 10^{22}$
47	1.739 ± 0.33	$3.10 \cdot 10^{22}$
49	1.875 ± 0.43	$2.40 \cdot 10^{22}$

* Molecular number densities up to 43 km were calculated using the Crawley 2300 GMT January 12th radiosonde and the West Geirinish January 17th rocketsonde. Average differences between these values and the U.S.S.A. is 5%. U.S.S.A. was used above 43 km.

TABLE 2

THE EFFECT OF THE ASSUMED REFRACTIVE INDEX ON THE DERIVED NUMBER DENSITIES

Model distribution	Number density of particles at 49 km with sizes between 0.1 and 1 μm. (cm^{-3})	
	$m = 1.4$	$m = 1.6$
Haze H	0.15	0.12
Power law, $\nu = 3$	0.036	0.0062
4	0.14	0.036
5	0.32	0.14
6	1.8	0.79

FIGURE 1

PLOTS OF THE BACKSCATTER GAIN , G , AS A FUNCTION OF THE MIE SIZE PARAMETER ,α, FOR M=1.61 AND M=1.4821 (FROM KERKER 1969)

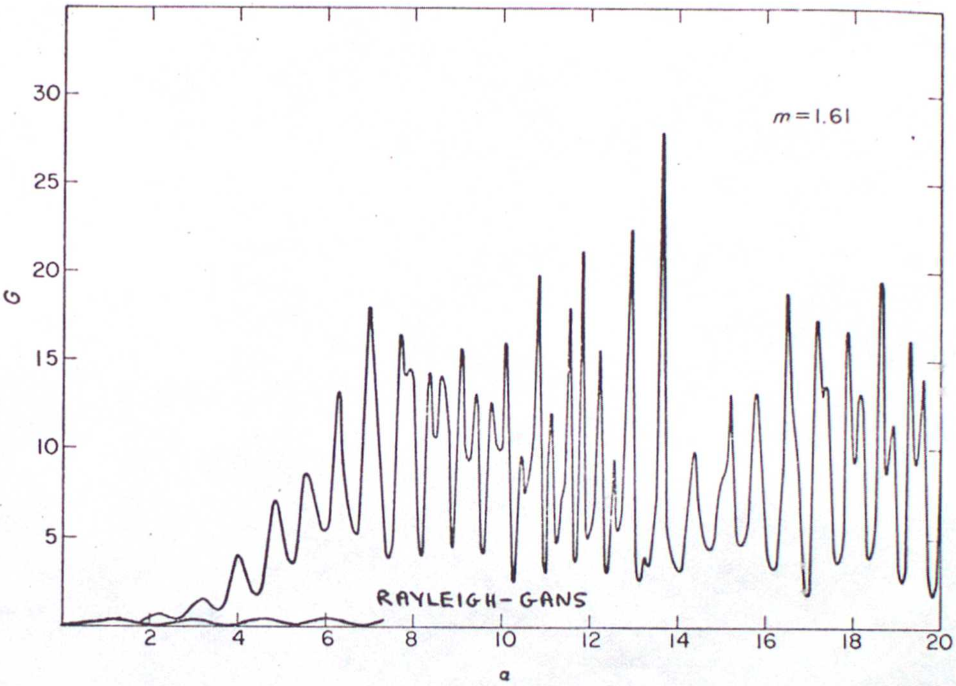

FIG. 4.31. Backscatter gain for dielectric sphere, $m = 1.61$.

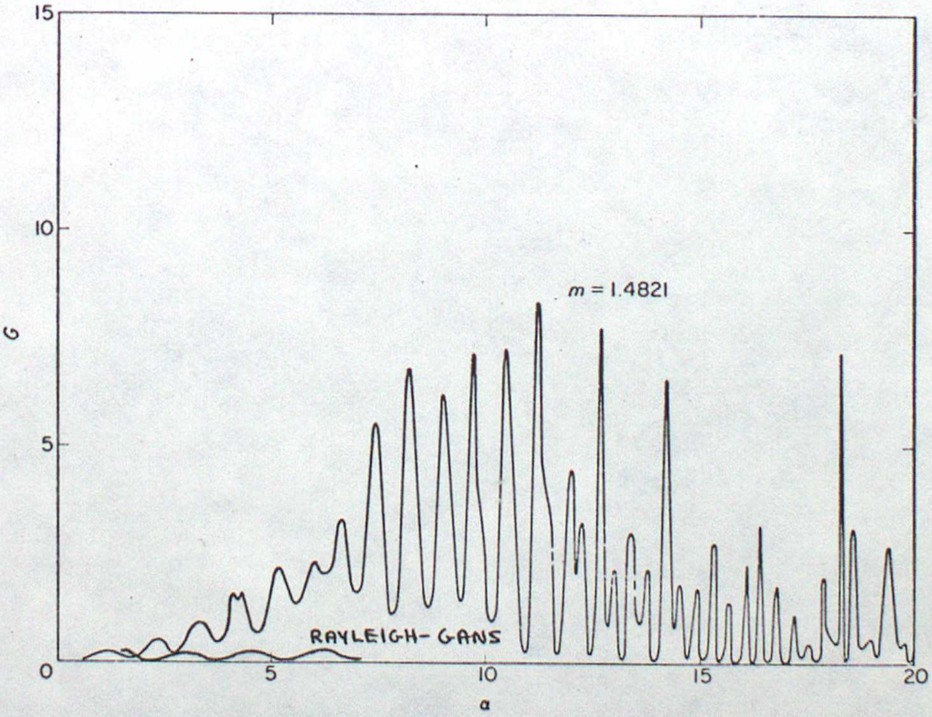

FIG. 4.32. Backscatter gain for dielectric sphere, $m = 1.4821$.

FIGURE 2 SIZE DISTRIBUTIONS MEASURED in situ BY VARIOUS INVESTIGATORS (FROM CADLE AND GRAMS (1975))

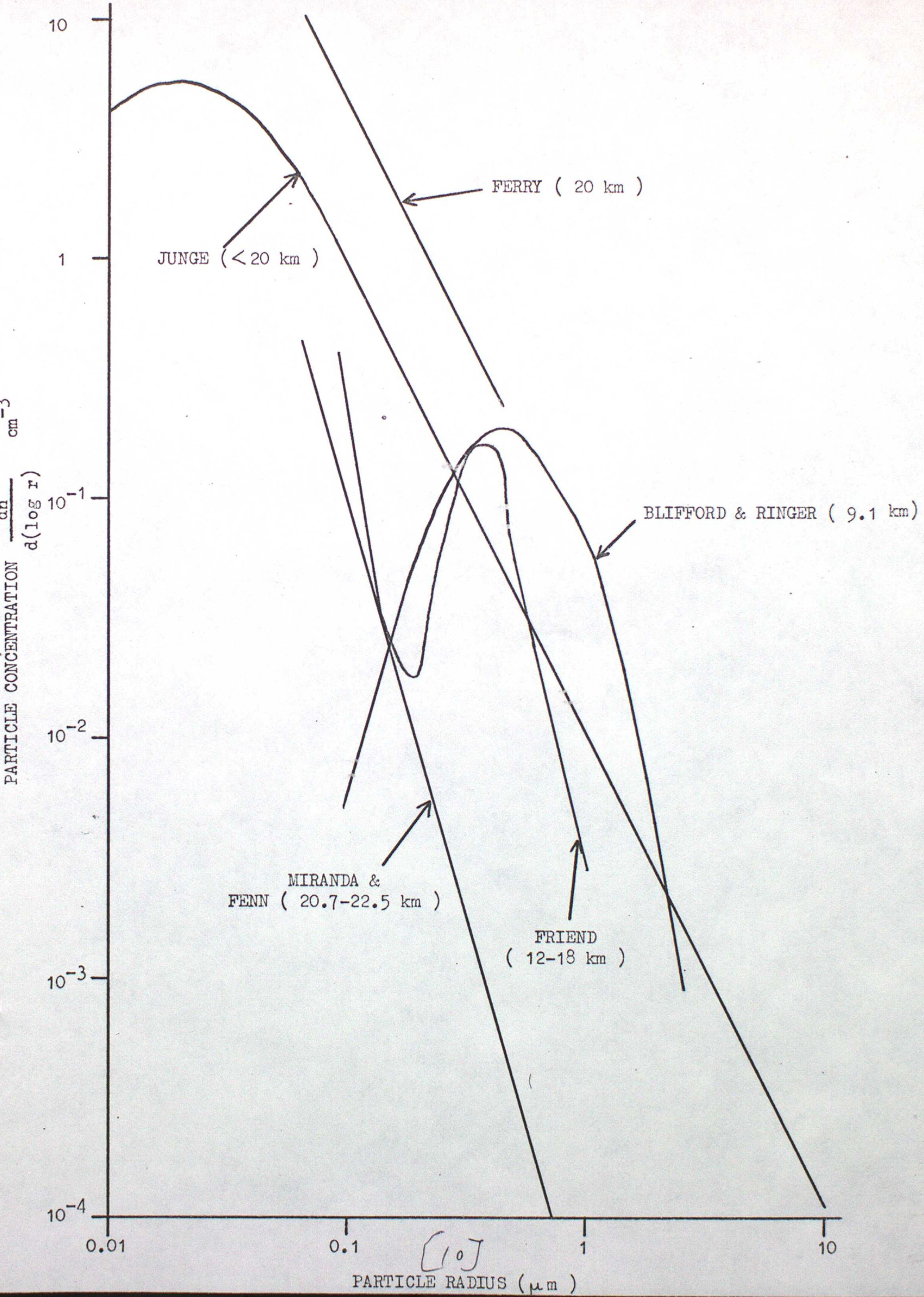

[10]

FIGURE 3 MODEL AEROSOL SIZE DISTRIBUTIONS

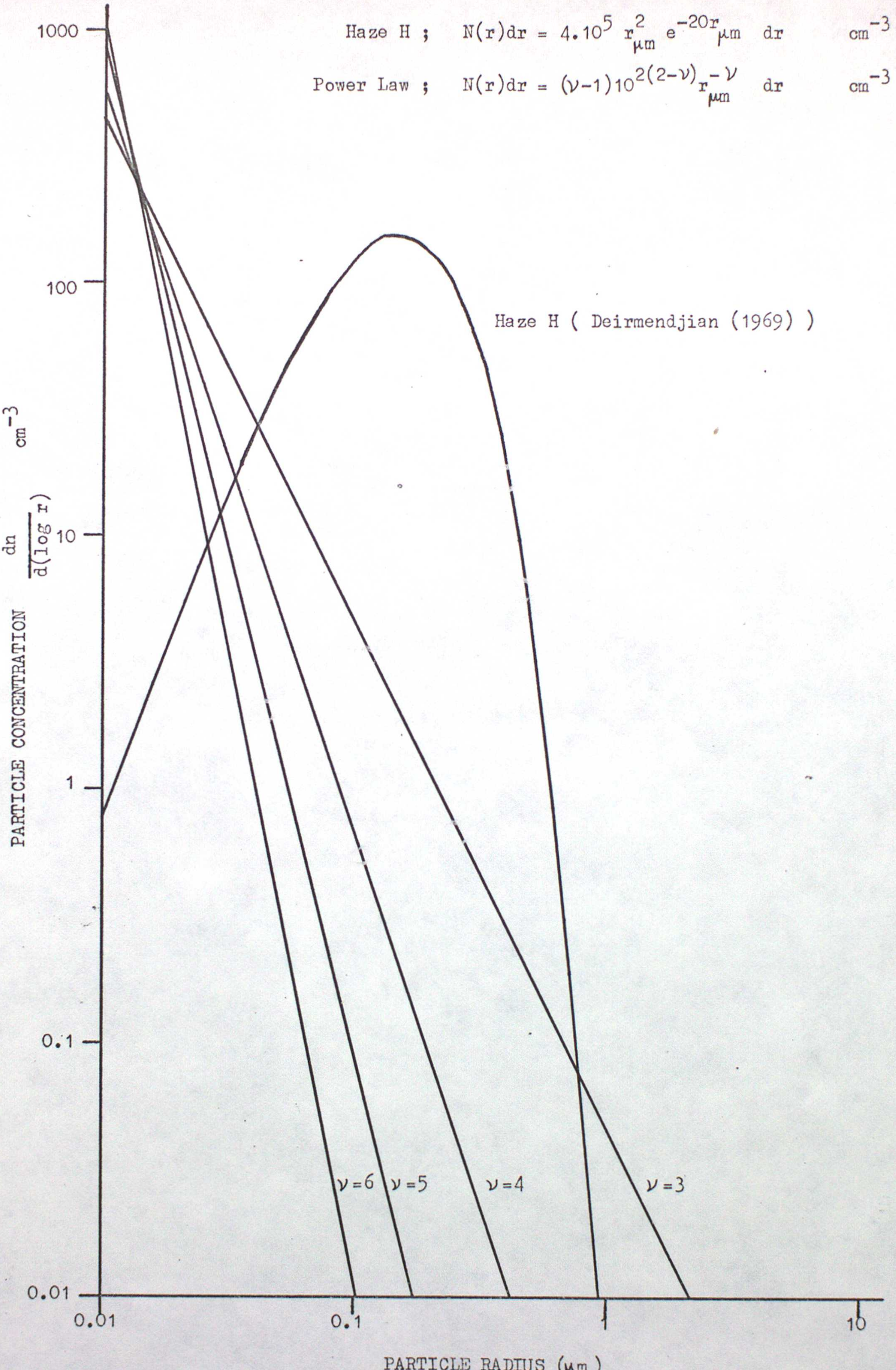

FIGURE 4

A(λ) AS A FUNCTION OF WAVELENGTH AND REFRACTIVE INDEX FOR THE HAZE H DISTRIBUTION

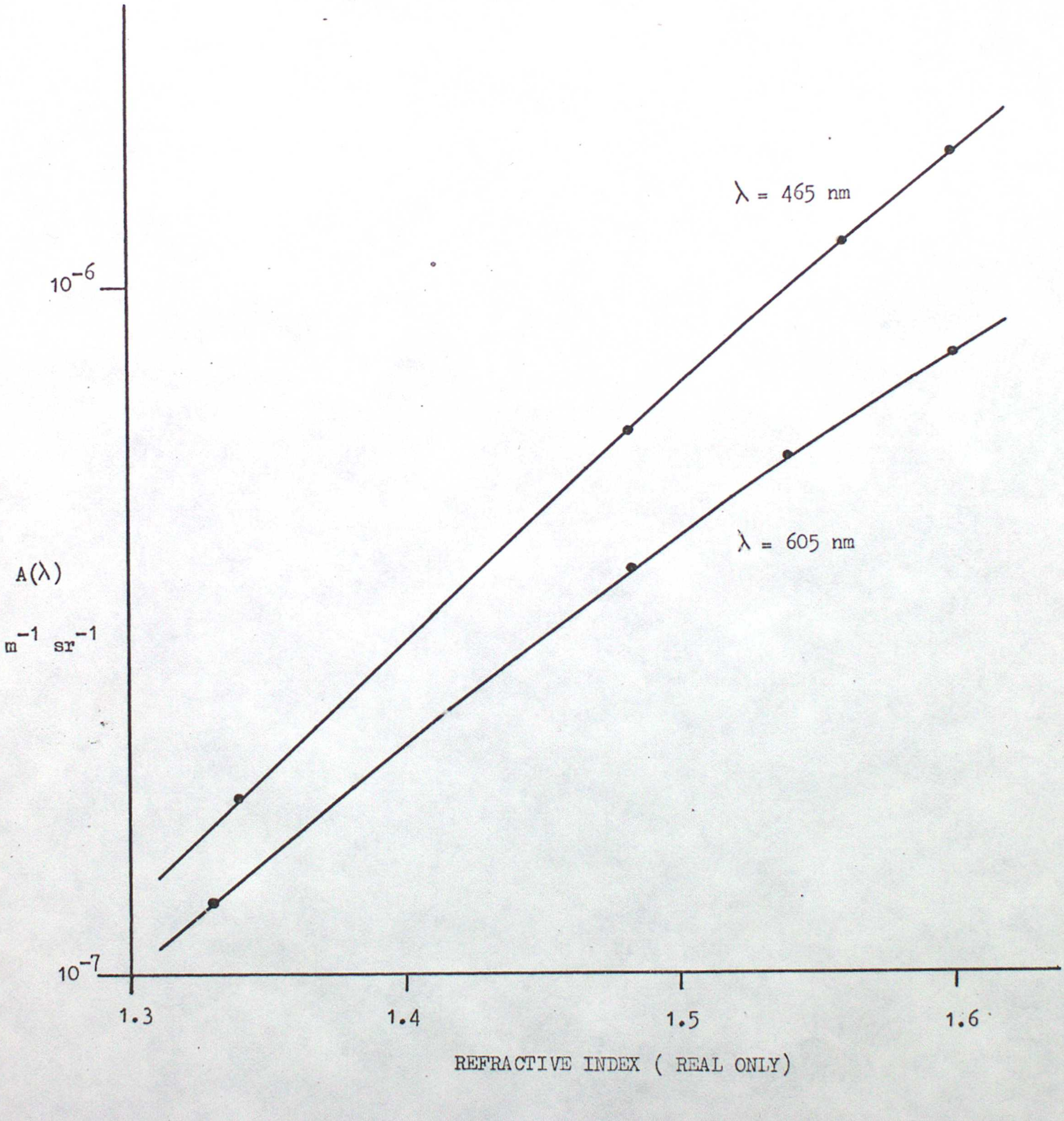

FIGURE 5 BEST FIT SIZE DISTRIBUTIONS AT 21 km

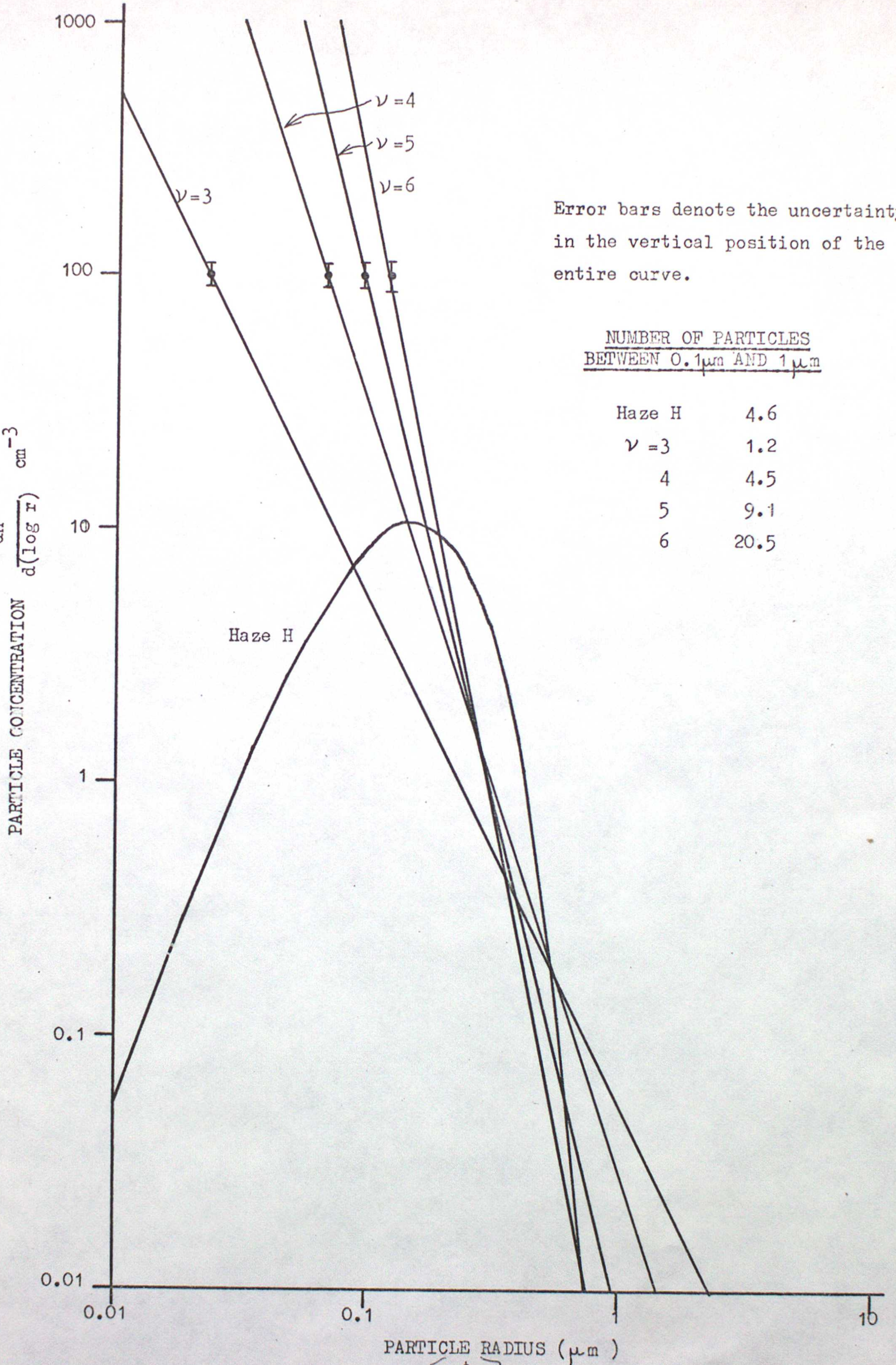

Error bars denote the uncertainty in the vertical position of the entire curve.

NUMBER OF PARTICLES BETWEEN 0.1 μm AND 1 μm

Haze H	4.6
$\nu = 3$	1.2
4	4.5
5	9.1
6	20.5

FIGURE 6 NUMBER DENSITY OF AEROSOLS WITH SIZES BETWEEN 0.1 μm AND 1 μm AS A FUNCTION OF HEIGHT (12/13-1-1975).

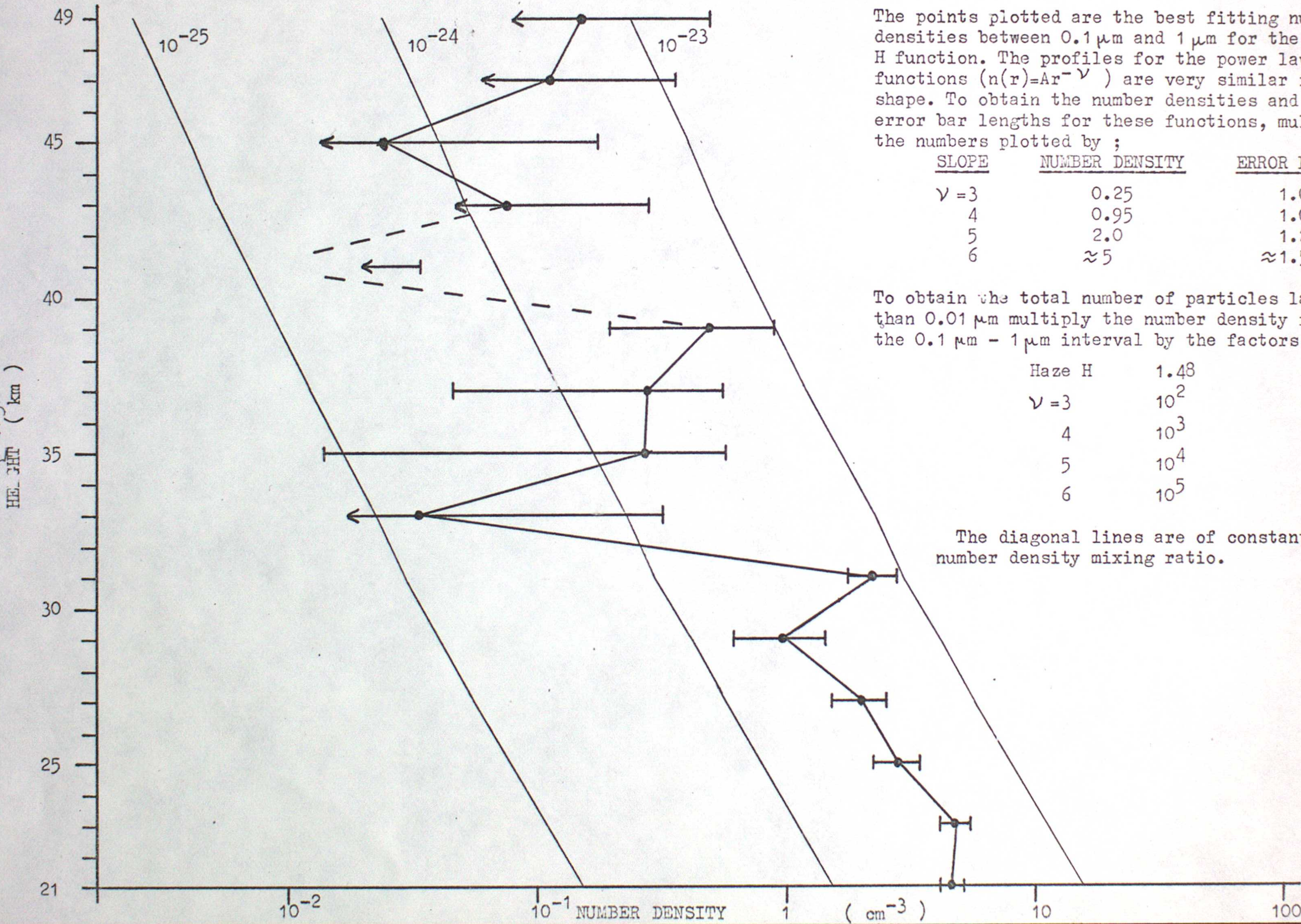

The points plotted are the best fitting number densities between 0.1 μm and 1 μm for the Haze H function. The profiles for the power law functions ($n(r)=Ar^{-\nu}$) are very similar in shape. To obtain the number densities and error bar lengths for these functions, multiply the numbers plotted by ;

SLOPE	NUMBER DENSITY	ERROR BARS
$\nu=3$	0.25	1.0
4	0.95	1.0
5	2.0	1.2
6	≈ 5	≈ 1.5

To obtain the total number of particles larger than 0.01 μm multiply the number density for the 0.1 μm - 1 μm interval by the factors ;

Haze H	1.48
$\nu=3$	10^2
4	10^3
5	10^4
6	10^5

The diagonal lines are of constant number density mixing ratio.